Analysis of variability in divergence and turn-over induced by three idealized convective systems with a 3D cloud resolving model

Edward Groot, Holger Tost
Institute of Atmospheric Physics, Johannes Gutenberg University, Mainz

1 Introduction

Error growth in numerical weather prediction models has widely been attributed to amongst others the simulation of (deep) moist convective processes and in recent years it has been found as important initial component of the chain of error growth in numerical weather simulations. Baumgart et al. (2019) found in a case study that error growth in ICON is initially largely attributable to the convection scheme, more so than to other model schemes. These errors saturate fast (< 12 h), ending up importantly affecting the near-tropopause region, where they spin-up divergent perturbations (subsequent day) which will then non-linearly grow and enter Rossby wave dynamics. Bierdel et al. (2017) and Bierdel et al. (2018) show that convective heat sources excite gravity waves and subsequent geostrophic adjustment can be a mechanism for a divergent flow perturbation (error) to enter the upper tropospheric balanced flow. Bierdel et al. (2017) show that linear superposition applies to such convectively induced pertubations or their errors. We investigate the magnitude and sensitivity of such an upper tropospheric (and lower stratospheric) divergent flow, by perturbing and altering some important processes.

It has been argued that deep convective processes can be accurately simulated at $dx \lesssim 250$ m (Bryan et al., 2003), as a large majority of the turbulence is then explicitly resolved. Hanley et al. (2014) and Stein et al. (2014) have shown that representation of intermediate to deep convection down to $r \approx 3$ km likely improves with $dx = 200$ m using the UK MetOffice model, but there are still caveats in the statistical representation compared to radar observations in multidimensional space. We simulate three idealized cases of convection in the cloud resolving model CM1 (Bryan, 2019) in LES mode.

2 Methods

CM1 configuration

- Grid: rectangular (aspect ratio 2.0) and cubic, dx 100-1000 m, vertical depth 20 km
- Duration 2 hours, $dt = 0.75$ s

Wind profiles #1, #2, #3

- Mean flow set such that domain propagates approximately with speed of convective system to increase residence time of flow perturbation inside domain

Initiation

- Default warm bubble initiation (#1 and #2): max. 0.67 K at $z \approx 1.35$ km
- Coldpool initiation (#3): max. -6 K at surface, western half of domain ("squall line")

Experiments

- Randomly generated perturbations for ensemble (9 members) to depth of the shear layers ($< 5\%$)
- Resolution (RES). Reference run and ensemble have $dx = dy = 200$ m, $dz = 100$ m.
- Latent heat of vaporisation adjusted (LV) by -40, -20, -10, +10 and +20% (altered ambient stratification acts similarly).
- Vertical advection of zonal and meridional momentum (VAUV) adjusted by -100, -50, -20 and +50% (artificially adapted convective momentum transport).
- Vertical advection of water vapor (VAQ) (-20 and +20%) for the effect of altered energy (re-)distribution.

Diagnostics (Horizontal) divergence (HDIV) has been derived from velocity fields using finite differences on grid points. Moist static energy (MSE) has been computed from potential temperature and water vapor mixing ratio. For the diagnosis of VAUV we implemented a diagnostic in the model code, without (the indirect) divergence contribution.

Region selection for budget calculations We average HDIV, mean condensation rate (COND), VAUV and ΔMSE over an area and selected time t, including most of the region with gravity wave activity excited. These gravity waves leave the model domain during the simulation (convective initiation in the first hour, C up to about 30 m/s).

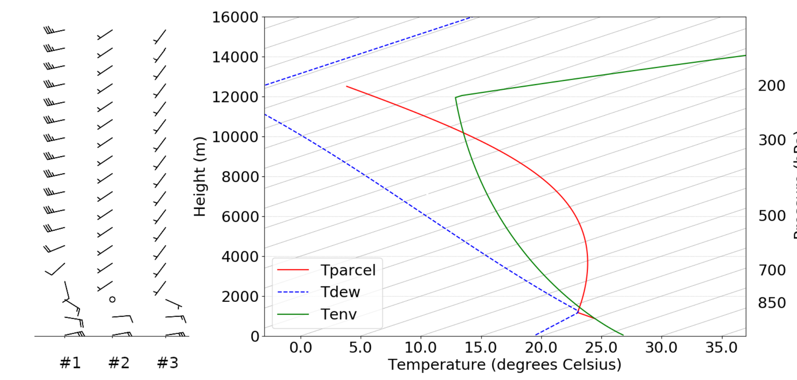

Initial environmental temperature (green) and dew-point (blue) profile and profile of a parcel forced upward without mixing (red). The wind profiles are shown on the left.

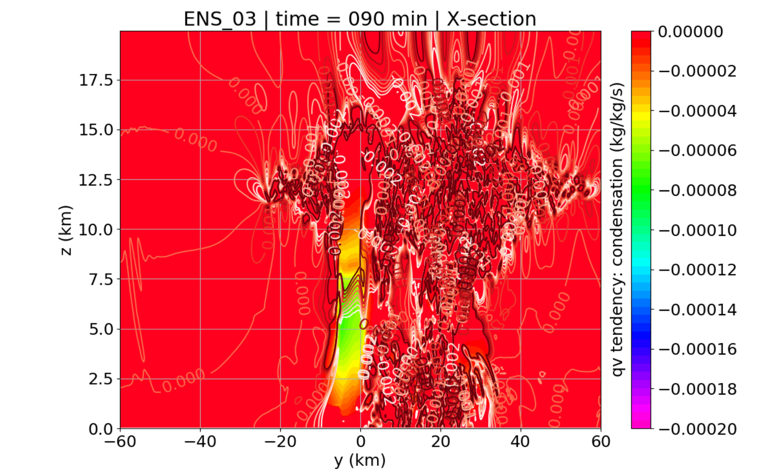

Vertical cross section (y-z plane) of condensation rate (colors) and isolines of horizontal divergence in brown (convergence: pink, per $5e^{-4}$ s^{-1}) through the cell core after 90 minutes for #1 (ensemble member 3).

4 Discussion

In line with findings by Hanley et al. (2014) with the UK MetOffice model, the quantities represented in Figure "Y" by high resolution simulations may underestimate realistic variability, but the relationship strongly suggests that the simulated systems behave very likely differently in converting latent heat to upper level divergence.

Collocated with Baumgart et al. (2019) we find strong manifestations of uncertainty in horizontal divergence in the near-tropopause region, for which the underlying reason is convective activity, consistently with the latter study. Combined with our methods, the methods of Baumgart et al. (2019) and Bierdel et al. (2018) can altogether potentially demonstrate that the mechanisms and uncertainty propagation explain an important portion of numerical uncertainty in evolution of the atmosphere. In terms of computational resources this would undoubtedly be a huge challenge.

References

Baumgart, M., Ghinassi, P., Wirth, V., Selz, T., Craig, G. C., & Riemer, M. (2019). Quantitative view on the processes governing the upscale error growth up to the planetary scale using a stochastic convection scheme. *Monthly Weather Review*, *147*(5), 1713–1731. URL https://doi.org/10.1175/mwr-d-18-0292.1

Bierdel, L., Selz, T., & Craig, G. (2017). Theoretical aspects of upscale error growth through the mesoscales: an analytical model. *Quarterly Journal of the Royal Meteorological Society*, *143*(709), 3048–3059. URL https://doi.org/10.1002/qj.3160

Bierdel, L., Selz, T., & Craig, G. C. (2018). Theoretical aspects of upscale error growth on the mesoscales: Idealized numerical simulations. *Quarterly Journal of the Royal Meteorological Society*, *144*(712), 682–694. URL https://doi.org/10.1002/qj.3236

Bryan, G. (2019). Cm1 (model): version 19.8. URL https://www2.mmm.ucar.edu/people/bryan/cm1/

Bryan, G. H., Wyngaard, J. C., & Fritsch, M. J. (2003). Resolution requirements for the simulation of deep moist convection. *Monthly Weather Review*, *131*, 2394–2416.

Hanley, K. E., Plant, R. S., Stein, T. H. M., Hogan, R. J., Nicol, J. C., Lean, H. W., Halliwell, C., & Clark, P. A. (2014). Mixing-length controls on high-resolution simulations of convective storms. *Quarterly Journal of the Royal Meteorological Society*, *141*(686), 272–284.

Stein, T. H. M., Hogan, R. J., Hanley, K. E., Nicol, J. C., Lean, H. W., Plant, R. S., Clark, P. A., & Halliwell, C. E. (2014). The three-dimensional morphology of simulated and observed convective storms over southern england. *Monthly Weather Review*, *142*(9), 3264–3283.

3 Selected results

Region of budget calculations

$w_{tropopause}$ in three reference runs (only > 4 m/s colored). Black rectangles mark the areas selected for budget calculations. Left: #1, centre: #2, right: #3; identical areas case #1 and #2 and nearly identical total area for #3. Evaluation at $t = 90$ min (#1 and #2) and $t = 75$ min (#3, to limit boundary effects).

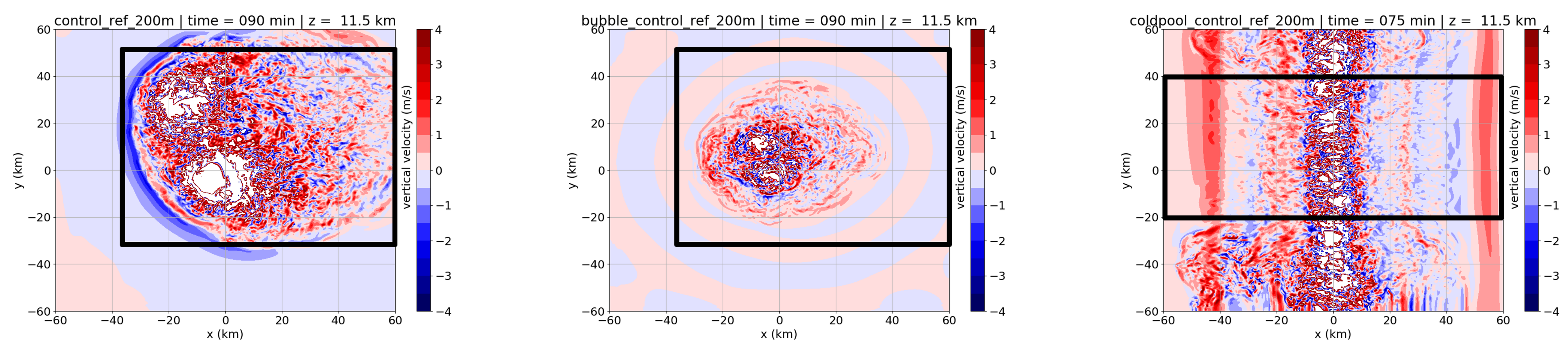

Experiment results

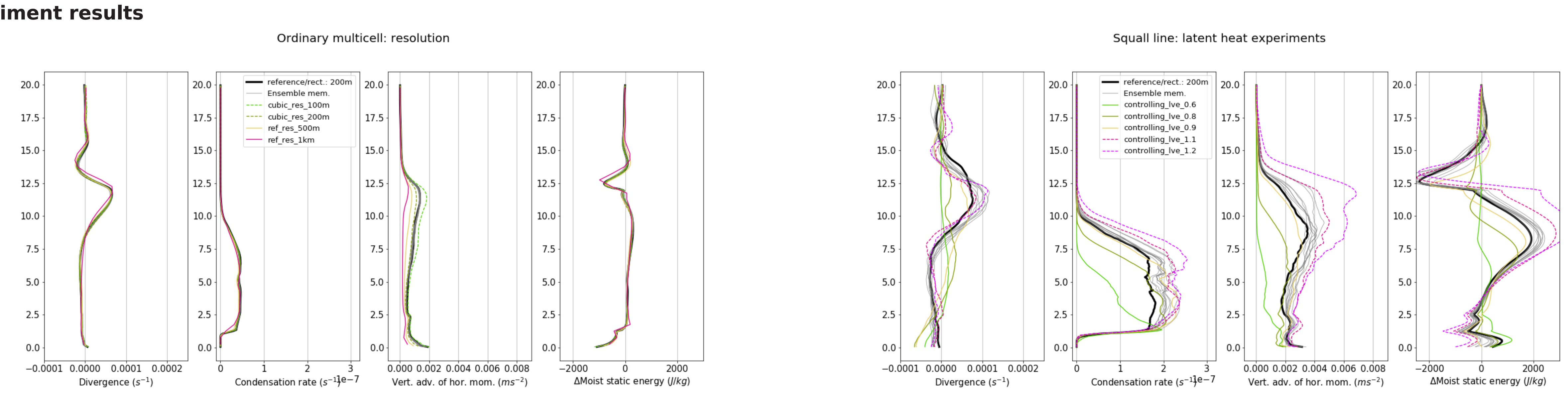

Budget profiles of HDIV at evaluation time t, COND up to t, mean VAUV up to t and ΔMSE up to t. Left: RES for #2. Right: LV with #3.

- Simulation at 1 km resolution (only #2 shown): suppressed extrema for all cases (under-resolved with fewer model levels); slight upward shift of profiles and stronger detrainment of stratospheric air near the tropopause (#2)
- Simulations with $dx = dy < 1000$ m have nearly converged, except for VAUV
- Despite near-convergence at high resolutions, squall line simulations reveal that the cubic grids are not always within ensemble spread (not shown)
- Explicitly resolved VAUV should indeed increase with spatial resolution (larger portion of the gradients are explicitly resolved)

- Large spread in squall line simulation (#3) among ensemble members in HDIV (much larger than in #1 and #2)
- Decreasing the latent heat constant significantly affects the magnitude (decrease) and distribution (lower altitude) of upper air HDIV, which is amplified by a reduced COND. The effect is even stronger for the other, less strongly forced (warm bubble), cases.
- Effect on VAUV among these simulations (cor)relates strongly with strength of convection and condensate mass

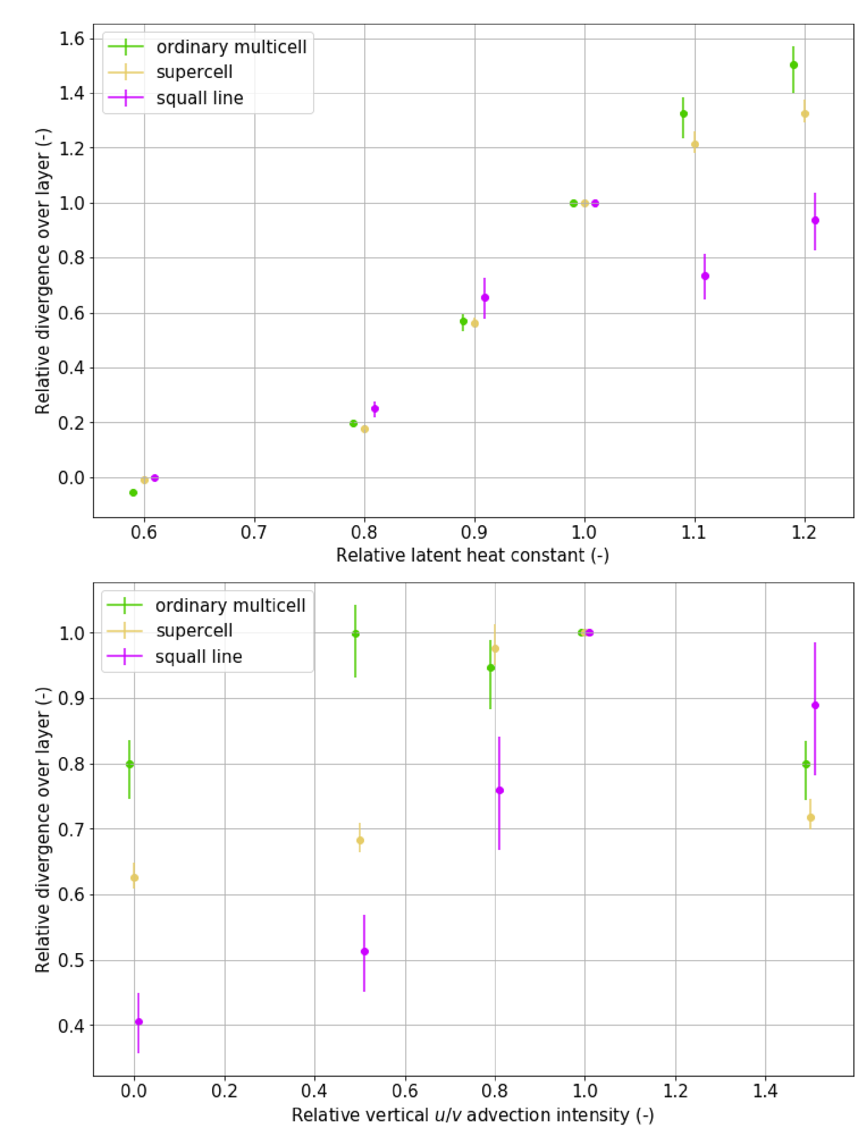

Top: dimensionless dependence of the 100-300 hPa layer divergence on latent heat constant; Bottom: idem for controlled VAUV.

- Direct feedbacks on the controlled process (momentum/water reservoirs)
- Structure/organisation and total area of convection are (often strongly) affected
- Effect on upper air HDIV not straightforward to attribute to the role of controlled processes

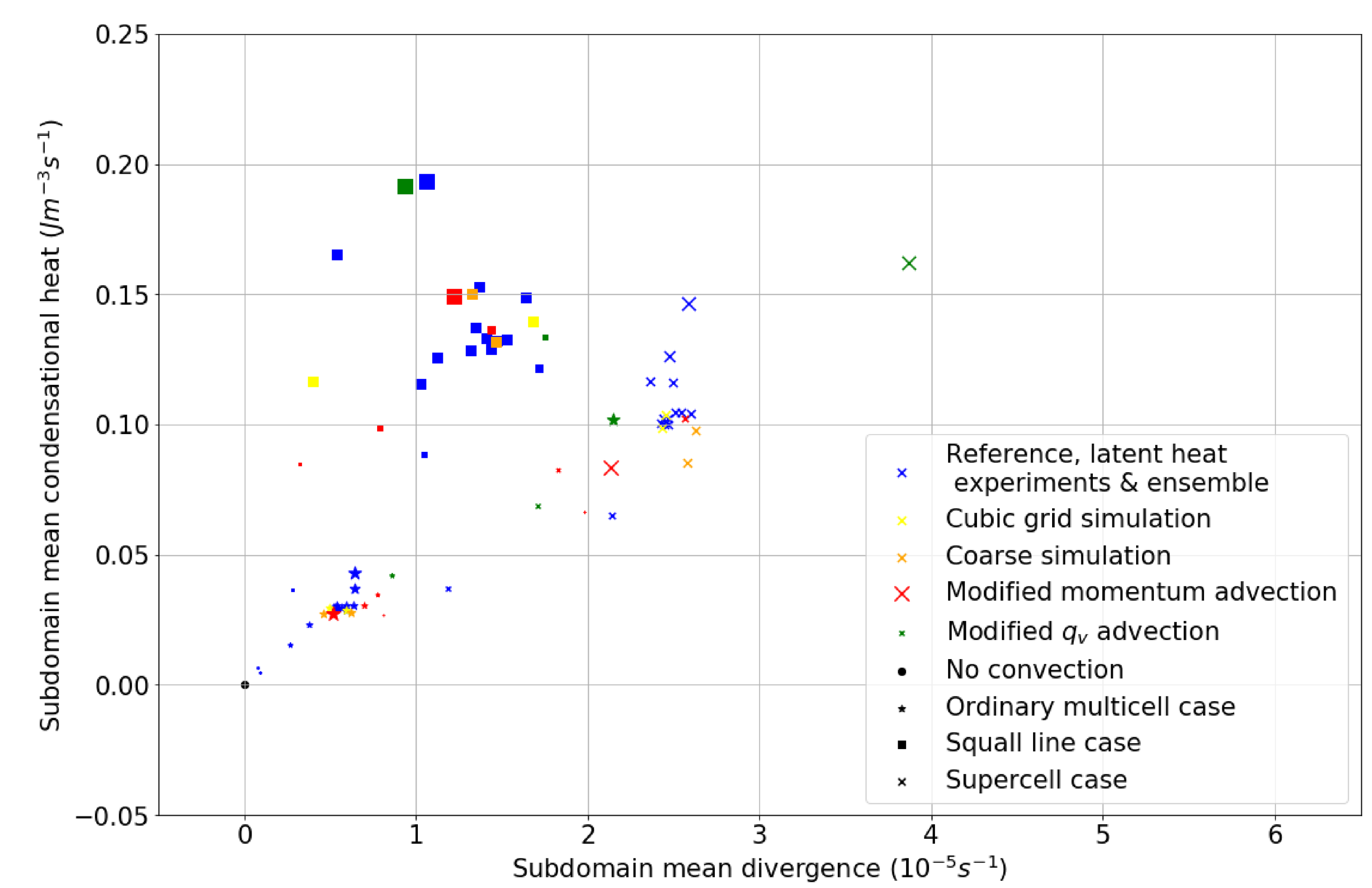

Density weighted mean HDIV ($z = 6 - 14$ km) at t as a function of latent heating up to t.

Strong dependence of divergence effects on mode of convection, next to latent heating, is also suggested. The Figure above ("Y") shows the relation between HDIV at 6-14 km and total condensational heat for all experiments. It suggests bimodal behavior with isolated convection leading to more HDIV for the same amount of condensational heat than squall lines. We suspect two main reasons for this:

- Squall line simulations are more efficient to redistribute MSE and thereby relax upper tropospheric instability (mainly 6-10 km), which would limit the expansion of air with condensational heat release compared to the other two cases (higher buoyancy gradients)
- Evaporation and sublimation of water and ice (after initial condensation) is slightly higher in squall line simulations (#1 and #2 ca. 20-30% versus #3 ca. 30-40%).